ARTICLE

Check for updates

Glacial mode shift of the Atlantic meridional overturning circulation by warming over the Southern Ocean

Akira Oka [1✉], Ayako Abe-Ouchi [1], Sam Sherriff-Tadano[1], Yusuke Yokoyama [1], Kenji Kawamura [2] & Hiroyasu Hasumi[1]

Abrupt climate warming events, known as Dansgaard-Oeschger events, occurred frequently during glacial periods, and are thought to be linked to changes in the Atlantic meridional overturning circulation. However, the mechanism responsible is not fully understood. Here, we present numerical simulations with a sea-ice coupled ocean general circulation model that systematically investigate the thermal threshold where deep water formation, and hence the overturning circulation, shift abruptly when the sea surface cools or warms sufficiently. Specifically, in our simulations where the magnitude of the sea surface cooling is changed separately or simultaneously in the Northern and Southern Hemispheres, a prominent threshold is identified when the Southern Hemisphere is slightly warmer than during glacial maxima. Abrupt mode changes of the Atlantic Meridional Overturning Circulation, like those during Dansgaard-Oeschger events, occur past a threshold in a transient simulation where the Southern Hemisphere is gradually warmed. We propose that the Southern Ocean plays a role in controlling the thermal threshold of the Atlantic Meridional Overturning Circulation in a glacial climate and that Southern Ocean warming may have triggered Dansgaard-Oeschger events which occurred with long interval.

[1] Atmosphere and Ocean Research Institute, University of Tokyo, Kashiwa, Chiba, Japan. [2] National Institute of Polar Research, Tachikawa, Tokyo, Japan.
✉email: akira@aori.u-tokyo.ac.jp

Greenland ice core data indicate the frequent occurrence of abrupt warming events during glacial periods, which are known as Dansgaard-Oeschger events (hereafter referred as DO events)[1,2] (Fig. 1a). Many hypotheses have been proposed to account for these events, and it is currently believed that they are related to changes in the Atlantic meridional overturning circulation[3,4] (AMOC). As demonstrated using a thermal bipolar seesaw model[5], the weakening (strengthening) of the AMOC is expected to cause cooling (warming) over the North Atlantic Ocean, followed by a delayed warming (cooling) over the Southern Ocean. Such a seesaw relationship is actually recorded in the Antarctic ice core data[6,7]; Antarctic temperatures rise during cold stadial periods in Greenland and begin to decline after abrupt warming occurs in Greenland[8]. This phase relationship between Greenland and Antarctica is apparent in Fig. 1, especially for long DO events (i.e., 8, 12, 14, 17, 19, 20, and 21) that are accompanied by large Antarctic warming events (i.e., A1–A7). In this study, we call these DO events type-L (marked with red-colored numbers in Fig. 1a). These type-L events are preceded by a period of gradual large warming in Antarctica and followed by a relatively longer warming period in Greenland (Fig. 1b). On the other hand, short DO events (i.e., 2–7, 9, 10, 11, 13, 15, 16, and 18) are here referred to as type-S (marked with blue-colored numbers in Fig. 1). Type-S DO events are preceded by smaller changes in Antarctica than type-L and are followed by a rapid return to stadial in Greenland (Fig. 1c). Albeit a less prominent signal than for the type-L DO events, the Antarctic changes that correspond to type-S DO events have been confirmed from high-resolution Antarctic ice core data[9]; these data support the idea that all DO events are related to changes in the AMOC.

Previous studies[10,11] have suggested that there are three modes of the AMOC in glacial climates: the interstadial, stadial, and Heinrich modes corresponding to a strong, weak, and halting AMOC, respectively. Rahmstorf[10] proposed that DO events occur when the AMOC shifts from a stadial or Heinrich mode to an interstadial mode. It is well known that changes in the AMOC mode can be triggered by a freshwater flux over the North Atlantic Ocean[12,13], which causes the AMOC to weaken and eventually stop. Geological data have recorded the occurrence of very large icebergs being discharged into the North Atlantic Ocean (Heinrich events[14]), providing further evidence in support of this scenario, because melting icebergs produce large freshwater inputs to the ocean. Freshwater forcing has consequently been recognized as an important factor for triggering DO events. However, the relationship between freshwater forcing and the AMOC is not clear because a freshwater input itself leads to weakening of the AMOC and thus is not a direct reason for its strengthening. In addition, proxy data indicate that the Heinrich events occurred during the stadial periods (i.e., during a weak AMOC), which suggests the possibility that the Heinrich events did not force the AMOC but instead occurred as a result of the AMOC weakening[15]. Therefore, another factor different from the freshwater forcing may be required to understand the mechanism responsible for DO events.

Besides freshwater fluxes, previous researches[16,17] have suggested that a gradual warming during deglaciation may be able to induce an abrupt resumption of the AMOC and cause an abrupt warming during the Bolling-Allerod period (B/A warming, marked as 1 in Fig. 1a). Similar mechanisms may also be operating in DO events. We previously proposed the existence of the thermal threshold in the AMOC during glacial climate periods[18,19]; i.e., the drastic changes in deep-water formation and in the AMOC can occur solely owing to surface cooling or warming, without requiring freshwater forcing. Those studies emphasized the importance of the surface conditions in the North Hemisphere[20,21]; the surface cooling or warming controls whether the sea ice covers or uncovers the convection area in the North Atlantic[22,23], which in turn controls the AMOC by affecting heat exchange between the atmosphere and ocean. On the other hand, several studies have highlighted the role of the Southern Hemisphere processes; the AMOC can be controlled by the temperature and brine formation in the Southern Ocean[24–26]. Previous studies have pointed out possible roles from both the Northern[27] and Southern Hemispheres[28], but their individual roles have not been systematically investigated together. In this study, by using the climate model simulations, we have systematically investigated the glacial structure of the AMOC thermal threshold under various conditions in which the magnitude of the sea surface cooling is separately or simultaneously changed in the Northern and Southern Hemispheres in order to understand the individual hemispheric roles. Based on these modeling results and their comparison with ice core records, we propose that the crossing of the thermal threshold of the AMOC caused by gradual southern warming leads to a rapid strengthening of the AMOC and thus acts as a triggering mechanism for the onset of DO events, especially type-L DO events.

Results

Thermal threshold of the AMOC. To investigate the structure of the thermal threshold of the AMOC, we performed numerical simulations with a sea-ice-coupled ocean general circulation model (OGCM); the sea surface boundary conditions for the modern, glacial, and blended climates are specified by results from the MIROC-coupled climate model simulations[29,30]. For the modern thermal conditions, the maximum volume transport of the AMOC reaches 18 Sv ($1\,\mathrm{Sv} = 10^6\,\mathrm{m}^3\,\mathrm{s}^{-1}$; Fig. 2a) and it is nearly equivalent to the observed estimate for the present-day AMOC[31]. When we gradually change the thermal conditions from a modern to a glacial climate (the gray dots in Fig. 2d; the horizontal axis is a cooling factor fc defined in the Methods section below), a moderate cooling produces a stronger AMOC (the gray dots at fc = 0.2, 0.4, and 0.6 in Fig. 2d). Even under the thermal conditions that are nearly equivalent to the glacial climate (i.e., fc = 0.8, 1.0, and 1.2), the AMOC continues to be stronger than the modern climate; we interpret this state as an interstadial mode of the AMOC (see Fig. 2b; fc = 1.2). When additional cooling is applied, the AMOC suddenly weakens (fc = 1.4 and 1.6); we interpret this as a drastic shift to a stadial mode of the AMOC (see Fig. 2c; fc = 1.6). We previously demonstrated that this transition can be explained by the existence of the thermal threshold in the AMOC[18]. An interstadial mode of the AMOC is maintained by active deep-water formation in the Greenland and Irminger Seas, which is similar to the modern climate. However, substantial cooling beyond the thermal threshold results in an extension of sea ice that completely covers the Greenland and Irminger Seas. This leads to a southward shift of the deep-water formation and a drastic change in the AMOC from a strong interstadial mode to a weak stadial mode[18,20,21].

We further analyzed the glacial structure of the AMOC thermal threshold by changing the thermal conditions separately in the Northern and Southern Hemispheres. When Northern Hemisphere cooling is applied to the modern AMOC with no change in the Southern Hemisphere, the AMOC simply strengthens from modern (fc = 0) to full-glacial (fc = 1.6) thermal conditions (the blue dots in Fig. 2d); a threshold behavior is not observed. However, when cooling is applied to the modern state only in the Southern Hemisphere, the AMOC gradually weakens between fc = 0 and fc = 1, and a sudden shift to the very weak AMOC is observed at fc = 1.2 (the red dots in Fig. 2d). This result indicates that the thermal threshold is located around approximately fc = 1.2 for this Southern Hemisphere cooling scenario.
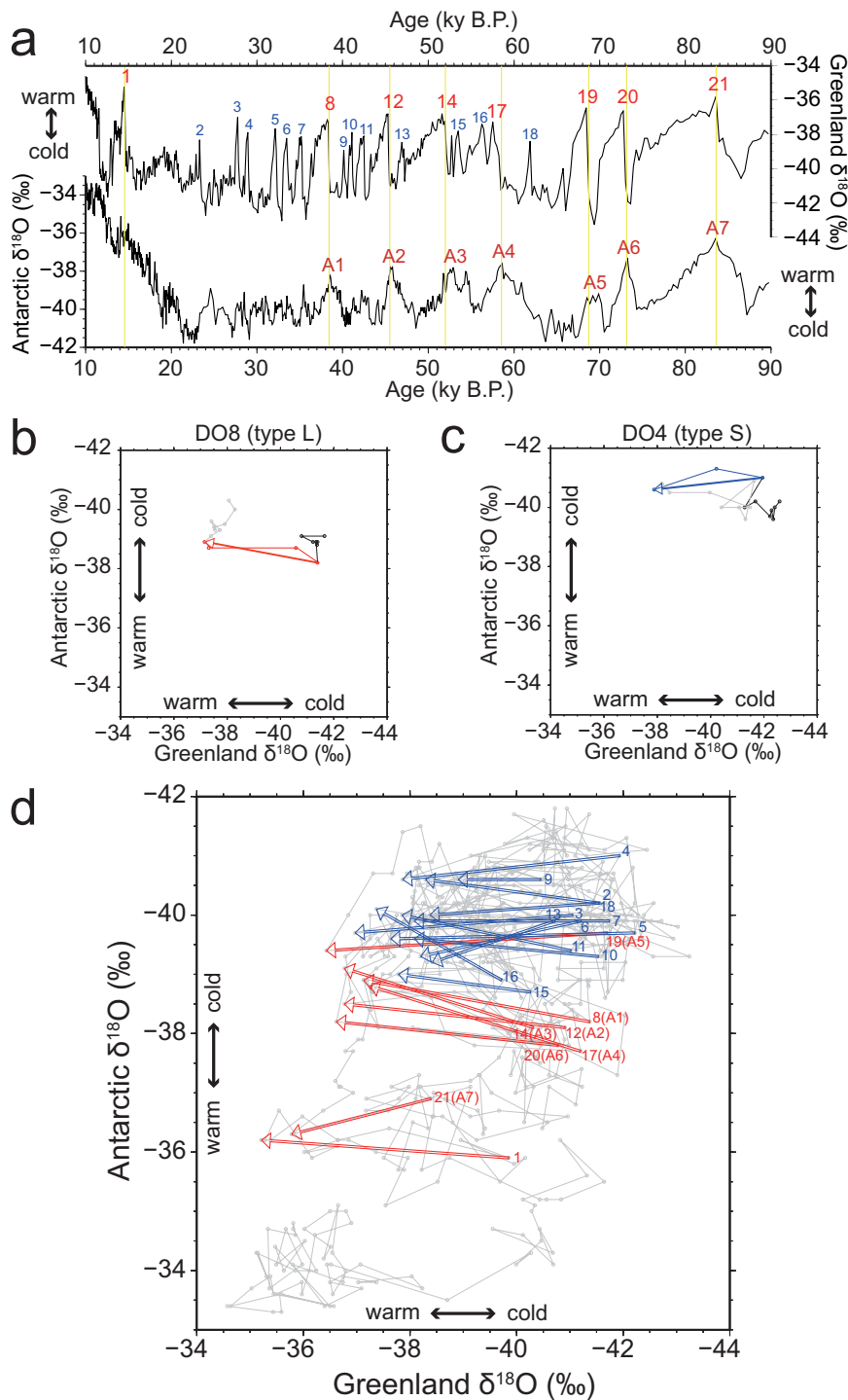
Fig. 1 Glacial air temperature record from the Greenland and Antarctic ice core data. a The time series of the oxygen isotope d^{18}O were obtained from the Greenland GISP2[2] (top) and Antarctic Byrd[6] ice core data (bottom). The timescales are synchronized using the methane concentrations[7]. The numbers represent Dansgaard-Oeschger (DO) events, with red-colored numbers corresponding to the type-L one. The numbers A1–A7 correspond to Antarctic-warming events. **b** Phase diagram for DO event 8 (a type-L DO event), where the d^{18}O values from Greenland and Antarctica are plotted along the horizontal and vertical axes, respectively. The black, red, and gray circles represent data for 1000 years before the event, during the event, and 1000 years after the event, respectively. Temporally adjacent data (circles) are connected to each other through lines. The DO event is highlighted by the red arrow; the starting and ending points of the arrow represent the event onset and peak of the event, respectively. **c** The same as **b** except for DO event 4 (a type-S DO event), in which the event is colored blue. **d** The same as **b** except for all of the DO events, in which all of the ice core d^{18}O data are plotted with gray circles; the type-L and type-S DO events are represented by the red and blue arrows, respectively.
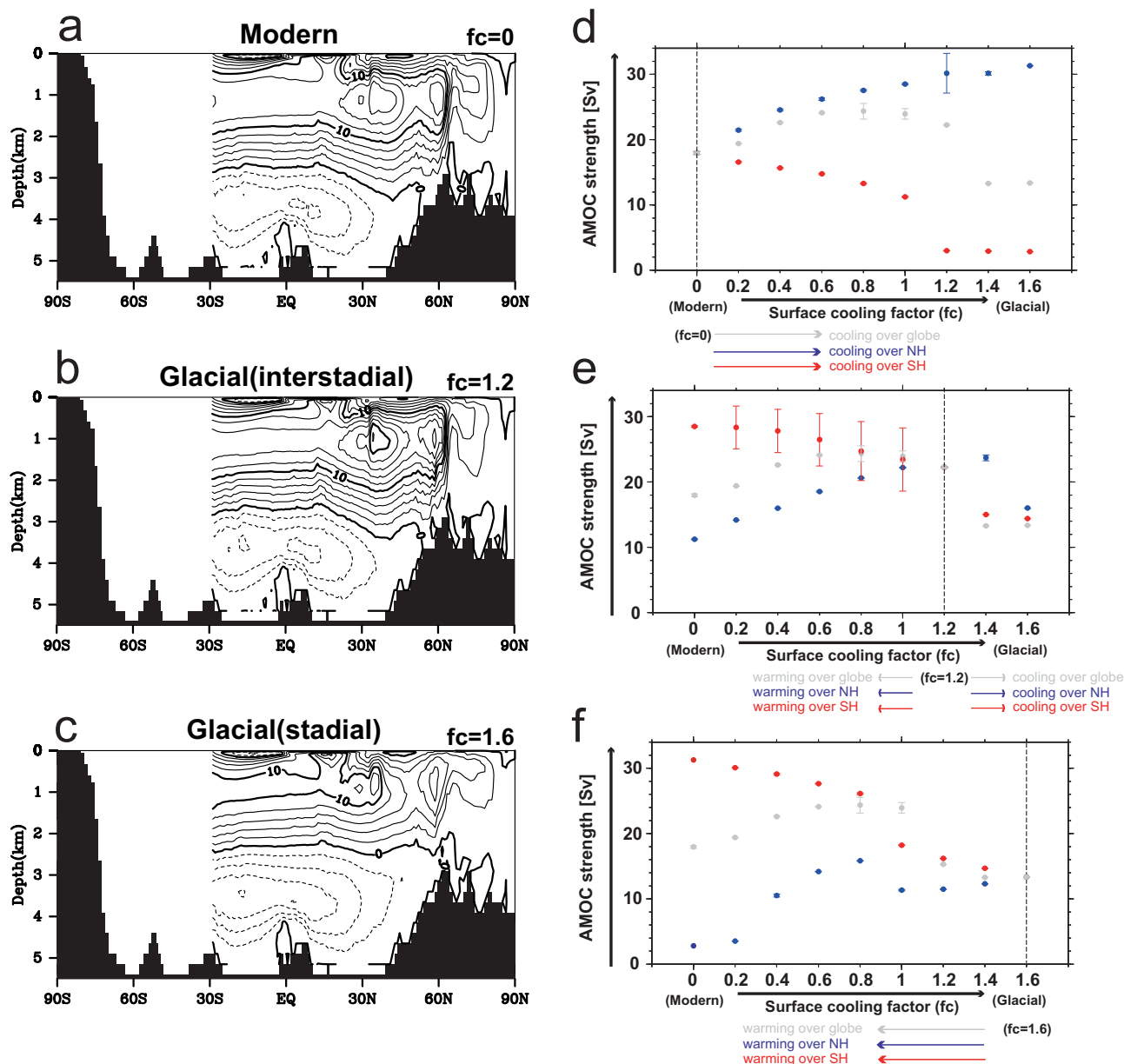
Fig. 2 Results of the ocean general circulation model simulations of the AMOC. a The simulated Atlantic meridional overturning circulation (AMOC) under modern thermal conditions (the cooling factor fc is 0). The contour interval is 2 Sv (1 Sv = 10^6 m³ s⁻¹). **b** The same as **a** except for the interstadial glacial state (fc = 1.2). **c** The same as **a** except for the stadial glacial state (fc = 1.6). **d** The maximum value of the AMOC is plotted against fc for a case in which the cooling is applied to the modern AMOC (fc is increased from fc = 0). The gray, blue, and red dots indicate the results in which the cooling is applied over the entire globe, only in the Northern Hemisphere, and only in the Southern Hemisphere, respectively. As inter-decadal oscillations in the AMOC are found in some simulations, error bars indicate the standard deviations of the oscillations. **e** The same as **d** except that the cooling/warming is applied to the interstadial AMOC (fc is increased/decreased from fc = 1.2). **f** The same as **d** except that the warming is applied to the stadial AMOC (fc is decreased from fc = 1.6).

Next, starting from an interstadial mode of the AMOC (fc = 1.2; Fig. 2b), we apply additional cooling separately in the Northern and Southern Hemispheres in the same manner. In this case (Fig. 2e), both scenarios (i.e., both Northern Hemisphere cooling and Southern Hemisphere cooling) can force the system to cross the threshold; a sudden shift to a weaker AMOC is observed at fc = 1.6 and fc = 1.4 for northern and southern cooling, respectively (the blue and red dots, respectively, in Fig. 2e). These results demonstrate that the condition for crossing the thermal threshold is related not only to the magnitude of global cooling but also to inter-hemispheric cooling patterns. Interestingly, Northern Hemisphere cooling can lead to either

strengthening or weakening of the AMOC depending on the base state of the climate. Northern cooling basically causes the AMOC to strengthen consistent with the increased density of the northern oceans[32] when the state is far from the thermal threshold (e.g., the blue dots in Fig. 2d). At the same time, if the state is close to the threshold (i.e., in a colder climate), northern cooling can also cause a drastic weakening of the AMOC by covering the deep-water formation region with sea ice (e.g., the blue dots in Fig. 2e). The response of the AMOC to Southern Hemisphere cooling also depends upon whether the system crosses the thermal threshold or not. When the state is far from the thermal threshold, southern cooling leads to a gradual

weakening of the AMOC. However, when the system crosses the thermal threshold of the AMOC by the further southern cooling, our result clearly demonstrates that the weakening of the AMOC occurs drastically.

We performed a similar analysis by applying surface warming to a stadial mode of the AMOC (fc = 1.6; Fig. 2c). As expected, the stadial AMOC further weakens in response to a moderate surface warming in the Northern Hemisphere (the blue dots at fc = 1.4, 1.2, and 1; Fig. 2f); this response is consistent with the decrease of surface north-south density gradient[32]. When we apply larger warming, a resumption of the AMOC is observed at fc = 0.8; this indicates that the thermal threshold exists between fc = 0.8 and fc = 1. After this resumption, the AMOC weakens again with further surface warming over the Northern Hemisphere (the blue dots at fc = 0.6, 0.4, 0.2, and 0; Fig. 2f). In contrast, the stadial AMOC gradually strengthens with surface warming over the Southern Hemisphere (the red dots at fc = 1.4, 1.2, and 1; Fig. 2f); this gradual strengthening of the AMOC is also consistent with the decrease of the surface north-south density gradient[32] but several processes are involved and will be discussed in Discussion section. Interestingly, more drastic strengthening of the AMOC is observed at fc = 0.8. This drastic strengthening again is related to the thermal threshold; the signal of the surface warming in the Southern Hemisphere is advected northward in the interior ocean from the Southern to the Northern Hemispheres, and it causes drastic changes in the deep-water formation in the Greenland and Irminger Seas. Although both northern and southern warmings cause abrupt strengthening of the AMOC, an important finding here is that the response of the AMOC depends on the hemispheric warming scenario.

Role of thermal conditions over the Northern and Southern Hemispheres. To extensively investigate the thermal conditions that are required for the appearance of the AMOC thermal threshold, we performed >81 numerical simulations by changing the thermal conditions over the Northern and Southern Hemispheres either separately or concurrently. We summarize the results of these simulations in Fig. 3a, where the simulated maximum value of the AMOC is shown as a function of the cooling factors in the Northern Hemisphere (fc$_N$, lateral axis) and that in the Southern Hemisphere (fc$_S$, vertical axis). As multiple equilibria associated with the thermal threshold are found in some parameter ranges, small colored squares are also shown in the figure; they correspond to the interstadial value in a multiple-equilibrium regime (see Supplementary Text for discussion of multiple equilibria). The results show that the AMOC thermal threshold appears ubiquitously when the climate is slightly warmer than a full-glacial climate (highlighted by the white lines in Fig. 3a). If we focus on the amplitude of the AMOC strengthening after crossing the threshold, we also confirm that its amplitude tends to be larger when the Northern Hemisphere is close to full-glacial conditions and the Southern Hemisphere is slightly warmer than full-glacial conditions (e.g., fc$_N$ is around 1.4 and fc$_S$ is between 0.8 and 1 in Fig. 3a). This suggests that a gradual warming in the Southern Hemisphere from a full-glacial climate can cause a substantial strengthening of the AMOC, which is explained by the existence of such a prominent thermal threshold.

The results presented here give an important insight into the interpretation of ice core data and have beneficial implications for mechanism of DO events. The Greenland and Antarctic ice core data indicate that the onsets of type-L DO events occur at a common thermal condition, in which Greenland is in a nearly a full-glacial state and Antarctica is slightly warmer than a full-glacial state (the starting points of the red arrows in Fig. 1d; this feature is also confirmed from more recent ice core records[33],
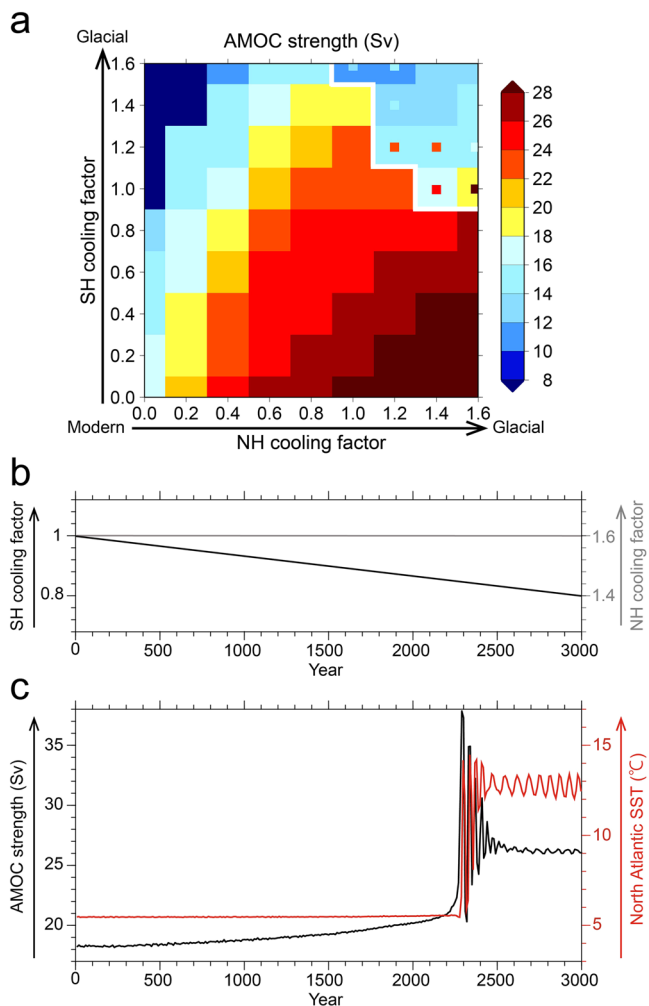
Fig. 3 The glacial structure of the AMOC thermal threshold. a The maximum value of the Atlantic meridional overturning circulation (AMOC) under various thermal conditions between the modern and full-glacial climates. The value on the horizontal (vertical) axis represents the cooling factor fc for the Northern (Southern) Hemisphere. The AMOC thermal threshold is highlighted by a white line. Note that multiple equilibria of the AMOC are found near the thermal threshold; the value that corresponds to the stadial mode of the AMOC is shown, while the value for interstadial AMOC is indicated by the colors of the small squares. **b** The specified time series of the cooling factor fc in our transient simulation. The black line represents the Southern Hemisphere (SH) cooling factor (i.e., fc$_S$), and the gray line represents the Northern Hemisphere (NH) cooling factor (i.e., fc$_N$). **c** The simulated time series of the maximum value of the AMOC (black line) and sea surface temperature in the North Atlantic (red line) in our transient simulation. For red line, we plotted the sea surface temperature at (42°W, 39°N) where the largest temperature changes are simulated.

shown in Supplementary Fig. 1). We propose that these climate conditions correspond to thermal conditions in which the prominent thermal threshold of the AMOC is located as shown in our simulations (Fig. 3a; the white line where fc$_N$ is around 1.4 and fc$_S$ is between 0.8 and 1). Given the existence of this thermal threshold, gradual warming in the Southern Hemisphere can lead to a substantial strengthening of the AMOC as a result of the crossing of this threshold. As all the type-L DO events are preceded by warming in Antarctica (Fig. 1a, b), the existence of the AMOC thermal threshold gives clear explanation about the

occurrence of type-L DO events (compare Fig. 1d with Fig. 3a). The mechanism proposed here may also explain why type-L DO events are only found during the earlier stages of the last glacial climate (before 35 ka) and not during the full-glacial period (35–20 ka); the climate is close to the AMOC thermal threshold before 35 ka, whereas the Southern Hemisphere becomes too cold to cross this threshold around 35–20 ka.

Transient simulation. To provide a further demonstration of the role of the thermal threshold as a possible explanation for the onset of the DO events, we performed a transient simulation in order to focus on the transient response of the AMOC rather than its steady-state response. In this transient simulation, the gradual warming of the Southern Hemisphere was applied to a stadial AMOC; from the stadial state ($fc_N = 1.6$ and $fc_S = 1.0$), we decreased fc_S linearly from 1.0 to 0.8 over 3000 years while maintaining fc_N at 1.6 (Fig. 3b). The simulated time series of the AMOC strength (the black line in Fig. 3c) indicates that an abrupt strengthening of the AMOC took place at around 2300 years, where the system crossed the threshold and the AMOC shifted from a stadial to an interstadial mode. The strengthening took place on a timescale of less than several decades and very large abrupt warming of sea surface temperature in the North Atlantic (a warming of 7.5 °C per decade; the red line in Fig. 3c) that is comparable to the DO events[34,35] was also reproduced in our simulation. Although an initial slowdown of the AMOC was required to reproduce the recovery/strengthening of the AMOC in previous freshwater hosing simulations, it is worthy note that the AMOC had nearly the same amplitude as in the present-day state before the strengthening occurred in our simulation.

Discussion

We showed that warming over the Southern Hemisphere can force the system to cross the thermal threshold and cause the AMOC mode shift (Fig. 3). In this section, we discuss about the dynamical processes by which the Southern Hemisphere warming caused the crossing of the thermal threshold. For this purpose, we first describe about the ocean state before and after the AMOC mode shift, respectively, in our transient simulation. Then, we discussed about the dynamic mechanisms by which the Southern Hemisphere warming leads to the AMOC mode shift.

Before the AMOC mode shift, the temperature of the upper ocean in the South Atlantic gradually becomes warmer (Supplementary Fig. 3g) as a result of the gradual surface warming in the Southern Hemisphere (the black line in Fig. 3b). Parts of the warming anomaly in the Southern Hemisphere are advected toward the North Atlantic in both upper (above 1000 m) and deeper (below 2000m) oceans (Supplementary Fig. 3g) associated with water mass formations of Antarctic Intermediate Water and Antarctic Bottom Water. The warming of deep water in the North Atlantic contributes to decreasing density (Supplementary Fig. 3e) and vertical stratification there, which appears to induce a gradual strengthening of the AMOC (the black line in Supplementary Fig. 3a; Supplementary Fig. 3c). As atmospheric freshwater forcing is not changed at all in our transient simulation, the changes in the surface freshwater flux come solely from sea-ice changes. The sea ice in the Southern Ocean is gradually reduced owing to surface warming (not shown), and this gradual sea-ice melting leads to an additional freshwater input around 70°S, which causes a decrease in the surface salinity there (Supplementary Fig. 3i). The low-salinity anomaly created in the Southern Ocean is advected toward the Atlantic Ocean via Antarctic Bottom Water formation; this deep-water freshening also contributes to the gradual strengthening of the AMOC by reducing the vertical stratification in the North Atlantic[26] in addition

to the above-mentioned deep-water warming shown in Supplementary Fig. 3g. As for the surface changes in the North Atlantic, our simulation shows an increase of density (Supplementary Fig. 3d, e), which comes from an increase in the salinity (Supplementary Fig. 3h, i). This increase of the salinity is associated with the strengthening of the AMOC; the salinity-feedback processes[36] are operating therein.

After a mode shift of the AMOC, the ocean state changes drastically from the state before the mode shift. The AMOC becomes significantly deep and strong (the black line in Supplementary Fig. 4a; Supplementary Fig. 4c). This mode change of the AMOC is associated with a shift of the deep convection sites (Supplementary Fig. 4b), as reported in our previous study[18]. Our previous study demonstrated that the thermal forcing (without freshwater forcing) can cause a shift of the deep convection sites, and in this study, we have newly reported that the thermal forcing only in the Southern Hemisphere (with no change in the Northern Hemisphere) can force the mode shift of the AMOC as a result of the gradual changes in the ocean state, as shown in Supplementary Fig. 3. The changes in the ocean state after the model shift of the AMOC are consistent with the significant strengthening of the AMOC; salinity in the northern North Atlantic including the Arctic Ocean becomes saltier (Supplementary Fig. 4h, i), which causes the higher density there (Supplementary Fig. 4d, e).

After analyzing the ocean states before and after crossing the thermal threshold described above, we here list up the processes that are responsible for the crossing of the thermal threshold caused by the Southern Hemisphere warming. By warming over the Southern Hemisphere, the following processes take place in the ocean: (1) the Southern Hemisphere warming leads to warming of deep water in the North Atlantic (due to transport from the Southern Ocean to the Atlantic deep ocean, associated with Antarctic Bottom Water formation; Supplementary Fig. 3g), (2) the Southern Hemisphere warming also leads to freshening of deep water in the North Atlantic (due to less sea-ice production in the Southern Ocean; Supplementary Fig. 3i), (3) the above two processes weaken the vertical stratification in the North Atlantic Ocean (Supplementary Fig. 3e), and (4) the weaker stratification enhances the deep-water convections in the North Atlantic Ocean and strengthens the AMOC (Supplementary Fig. 3b, c). Owing to the above-mentioned processes, the Southern Ocean Hemisphere warming causes the gradual strengthening of the AMOC. In addition, the following salinity-feedback processes take place: (5) the strengthening of the AMOC causes the increase of the surface salinity in the Atlantic Ocean (Supplementary Fig. 3h), and (6) the increase of the surface salinity further enhances the deep-water convections in the North Atlantic Ocean. This salinity feedback also contributes to the AMOC strengthening by enhancing the initial perturbations caused by the Southern Ocean warming. Finally, when the degree of the Southern Hemisphere warming becomes large enough for causing the shift of the deep convection sites, the crossing of the thermal threshold takes place: (7) as demonstrated in Oka et al.[18], the northward shift of deep convection sites suddenly takes place if the surface warming (i.e., the Southern Ocean warming, in this case) becomes large enough (Supplementary Fig. 4b), and (8) at the same time, the significant strengthening of the AMOC (i.e., the mode shift of the AMOC) takes place (Supplementary Fig. 4c) associated with the above-mentioned changes in the pattern of the deep-water formation.

In summary, before the AMOC mode shift (2100–2200 year; Supplementary Fig. 3), the gradual surface warming in the Southern Hemisphere causes the warmer and fresher deep water in the North Atlantic (Supplementary Fig. 3g, i), which reduces the vertical stratification there and causes the gradual strengthening of the AMOC. This gradual strengthening of the AMOC in

turn enhances the salinity transport toward the North Atlantic and leads to higher sea surface salinity over the North Atlantic (Supplementary Fig. 3h) via its salinity transport feedback[36], which further reduces the vertical stratification in the North Atlantic. The changes described above set up the ocean state required for the system to finally cross the thermal threshold of the AMOC (i.e., the rapid AMOC strengthening as a result of abrupt changes in the deep convection system in the North Atlantic[18]); when the degree of the Southern Hemisphere warming is large enough for causing the shift of the deep convection sites, the crossing of the thermal threshold and the mode shift of the AMOC take place (Supplementary Fig. 4).

As described above, the processes that control the mode change of the AMOC are not simple in that the gradual change of the AMOC before the model shift is involved with changes in both temperature and salinity. As both of them appear to affect the AMOC mode shift, further investigations will be required to obtain a more detail understanding of their individual roles in future studies.

Conclusions

At the beginning of this paper, we mentioned that another factor that is different from the freshwater forcing may be required to understand the mechanism responsible for DO events. This study proposed that crossing of the thermal threshold by a gradual southern warming can trigger an abrupt mode shift of the AMOC. It is important to emphasize that crossing the thermal threshold can occur even if no freshwater forcing exists. Therefore, our proposed mechanism may serve as one of the key processes of DO events that are different from the freshwater forcing. Although the actual DO events are related to complex interactions between the atmosphere, oceans, sea ice, and ice sheets[37,38], we believe that our findings are an important piece of the puzzle that is required to unravel this complex phenomenon and provide a step toward a fundamental understanding of the climate system.

Methods

Ocean model. The OGCM that is used in this study is COCO[39], which includes a dynamical sea-ice model[40]. The model adopts a horizontal curvilinear coordinate system, but we used the normal spherical coordinate system in this study. Isopycnal diffusion[41], isopycnal thickness diffusion[42], surface mixed layer[43] and bottom boundary layer[44] parameterizations are applied in the model. The ocean model is forced by surface heat, freshwater, and momentum fluxes. We obtained the atmospheric conditions that are required to specify these fluxes from the MIROC-coupled climate model simulations[45]: we used a medium-resolution version (an atmospheric resolution is T42L20, and the oceanic resolution is ~1°)[46,47]. In this study, modern (Control) and glacial (LGM) simulations are referenced; these results are the same as those reported in the Paleoclimate Model Intercomparison Project (PMIP) phase 2[48,49]. We employed the same resolution and model parameters as those of MIROC in our OGCM simulations. In this study, we performed time integration until a steady-state was obtained; time integration was continued at least for 1000 years. If 1000 years were not sufficiently long to obtain a steady-state (this happened near the thermal threshold), we prolonged the integration until the strength of the AMOC ceased to change.

Experimental design. To reproduce intermediate climate conditions between the modern and full-glacial climates, we introduced a cooling factor fc to specify the sea surface thermal conditions[18]. For example, the surface air temperature, which provides the sea surface thermal boundary condition for the OGCM simulations, is given by

$$T_A = T_{A(CTL)}(1 - fc) + T_{A(LGM)}fc \qquad (1)$$

where T_A is the air temperature, $T_{A(CTL)}$ is the air temperature from the MIROC Control simulation, and $T_{A(LGM)}$ is the air temperature from the MIROC LGM simulation. Note that the surface forcing used here is identical to that employed in our previous study[18], and the forcing anomaly between Control and LGM is shown in their Fig. 2. In addition to the thermal condition, the wind stress forcing is also changed to LGM condition here. Specifically, the experiment with various fc values in Eq. (1) is equivalent to HT-wind series simulation and fc = 0 case is identical to

LGM-wind simulation in our previous study (see their Table 1). Furthermore, as an extension from our previous study, we performed experiments where the values of the cooling factor fc were specified differently between the Northern and Southern Hemispheres; for example,

$$T_A = \begin{cases} T_{A(CTL)}(1 - fc_N) + T_{A(LGM)}fc_N, & \text{for } 0 < \text{latitude} < 90 \\ T_{A(CTL)}(1 - fc_S) + T_{A(LGM)}fc_S, & \text{for } -90 < \text{latitude} < 0 \end{cases} \qquad (2)$$

where fc_N is the cooling factor in the Northern Hemisphere and fc_S is the cooling factor in the Southern Hemisphere.

As in many other climate models[48], our original MIROC LGM simulation referenced here reached the stronger AMOC than the present-day climate, contrary to the weaker AMOC suggested from the proxy data (note that our updated MIROC model version can simulate the weaker LGM AMOC[20,30]). This means that our original LGM MIROC simulation is not cool enough to reach the thermal threshold, and this leads to the stronger AMOC than Control (i.e., fc = 1.0). However, applying further cooling can force the system to cross the threshold, leading to the weaker AMOC than Control (i.e., fc = 1.4 and 1.6). The location of the threshold depends on various aspects of the model bias (e.g., wind stress, surface temperature)[18,21], and we here regard the case fc = 1.0 as an interstadial glacial climate, although this was originally intended to reproduce the full-glacial climate in the MIROC simulation. Similarly, we regard the state before the system crosses the thermal threshold as a stadial glacial climate. Although the strength of the stadial AMOC is usually weaker than the modern AMOC, note that some of stadial AMOC cases simulated in our model become similar to—or sometimes slightly stronger than—the modern AMOC. Even in such a case, we use the term stadial if a state is located before the crossing of the thermal threshold in this study.

Data availability

Data presented in the figures are available at https://doi.org/10.5281/zenodo.5040210. The ice-core data used in Fig. 1 is available from Blunier and Brook[7].

Code availability

The information on COCO can be obtained from the web site (https://ccsr.aori.u-tokyo.ac.jp/~hasumi/COCO/) and readers are requested to contact the corresponding author if they wish to validate the model configurations and conduct replication experiments.

References

1. Dansgaard, W. & Johnsen, S. Evidence for general instability of past climate from a 250-kyr ice-core record. *Nature* **364**, 218–220 (1993).
2. Grootes, P. M., Stuiver, M., White, J. W. C., Johnsen, S. & Jouzel, J. Comparision of oxygen isotope records from the GISP2 and GRIP Greenland ice cores. *Nature* **366**, 552–554 (1993).
3. Clark, P. P. U. P., Pisias, N. N. G., Stocker, T. T. F. T. & Weaver, A. A. J. A. The role of the thermohaline circulation in abrupt climate change. *Nature* **415**, 863–869 (2002).
4. Menviel, L. C., Skinner, L. C., Tarasov, L. & Tzedakis, P. C. An ice–climate oscillatory framework for Dansgaard–Oeschger cycles. *Nat. Rev. Earth Environ.* https://doi.org/10.1038/s43017-020-00106-y (2020).
5. Stocker, T. T. F. T. & Johnsen, S. S. J. A minimum thermodynamic model for the bipolar seesaw. *Paleoceanography* **18**, 1–9 (2003).
6. Johnsen, S., Dansgaard, W., Clausen, H. & Langway, C. Oxygen isotope profiles through the Antarctic and Greenland ice sheets. *Nature* **235**, 429–434 (1972).
7. Blunier, T. & Brook, E. J. Timing of millennial-scale climate change in Antarctica and Greenland during the last glacial period. *Science* **291**, 109–112 (2001).
8. Members, W. D. P. Precise interpolar phasing of abrupt climate change during the last ice age. *Nature* **520**, 661–665 (2015).
9. Barbante, C. et al. One-to-one coupling of glacial climate variability in Greenland and Antarctica. *Nature* **444**, 195–198 (2006).
10. Rahmstorf, S. Ocean circulation and climate during the past 120,000 years. *Nature* **419**, 207–214 (2002).
11. Böhm, E. et al. Strong and deep Atlantic meridional overturning circulation during the last glacial cycle. *Nature* **517**, 73–76 (2015).
12. Rahmstorf, S. Bifurcations of the Atlantic thermohaline circulation in response to changes in the hydrological cycle. *Nature* **378**, 145–149 (1995).
13. Ganopolski, A. & Rahmstorf, S. Rapid changes of glacial climate simulated in a coupled climate model. *Nature* **409**, 153–158 (2001).
14. Heinrich, H. Origin and consequences of cyclic ice rafting in the northeast Atlantic Ocean during the past 130,000 years. *Quat. Res.* **152**, 142–152 (1988).

15. Bassis, J. N., Petersen, S. V. & Mac Cathles, L. Heinrich events triggered by ocean forcing and modulated by isostatic adjustment. *Nature* **542**, 332–334 (2017).
16. Knorr, G. & Lohmann, G. Southern Ocean origin for the resumption of Atlantic thermohaline circulation during deglaciation. *Nature* **424**, 532–536 (2003).
17. Obase, T. & Abe-Ouchi, A. Abrupt Bølling-Allerød warming simulated under gradual forcing of the last deglaciation. *Geophys. Res. Lett.* 2019GL084675 https://doi.org/10.1029/2019GL084675 (2019).
18. Oka, A., Hasumi, H. & Abe-Ouchi, A. The thermal threshold of the Atlantic meridional overturning circulation and its control by wind stress forcing during glacial climate. *Geophys. Res. Lett.* **39**, https://doi.org/10.1029/2012GL051421 (2012).
19. Marozke, J. A grip on ice-age ocean circulation. *Nature* **485**, 180–181 (2012).
20. Sherriff-Tadano, S. & Abe-Ouchi, A. Roles of sea ice–surface wind feedback in maintaining the glacial Atlantic meridional overturning circulation and climate. *J. Clim.* **33**, 3001–3018 (2020).
21. Sherriff-Tadano, S., Abe-Ouchi, A., Yoshimori, M., Oka, A. & Chan, W.-L. Influence of glacial ice sheets on the Atlantic meridional overturning circulation through surface wind change. *Clim. Dyn.* **50**, 2881–2903 (2018).
22. Li, C., Battisti, D. S. & Bitz, C. M. Can North Atlantic sea ice anomalies account for Dansgaard-Oeschger climate signals? *J. Clim.* **23**, 5457–5475 (2010).
23. Zhang, X., Lohmann, G., Knorr, G. & Purcell, C. Abrupt glacial climate shifts controlled by ice sheet changes. *Nature* **512**, 290–294 (2014).
24. Jansena, M. F. & Jansen, M. F. Glacial ocean circulation and stratification explained by reduced atmospheric temperature. *Proc. Natl. Acad. Sci. USA* **114**, 45–50 (2016).
25. Klockmann, M., Mikolajewicz, U. & Marotzke, J. The effect of greenhouse gas concentrations and ice sheets on the glacial AMOC in a coupled climate model. *Clim. Past* **12**, 1829–1846 (2016).
26. Buizert, C. & Schmittner, A. Southern Ocean control of glacial AMOC stability and Dansgaard-Oeschger interstadial duration. *Paleoceanography* **30**, https://doi.org/10.1002/2015PA002795 (2015).
27. Lohmann, J. Prediction of Dansgaard-Oeschger events from greenland dust records. *Geophys. Res. Lett.* **46**, 12427–12434 (2019).
28. Dima, M., Lohmann, G. & Knorr, G. North Atlantic versus global control on Dansgaard-Oeschger events. *Geophys. Res. Lett.* **45**, 12991–12998 (2018).
29. Hasumi, H. & Emori, S. *K-1 Coupled GCM (MIROC) Description* (K-1 Model Developers, 2004).
30. Kawamura, K. et al. State dependence of climatic instability over the past 720,000 years from Antarctic ice cores and climate modeling. *Sci. Adv.* **3**, 1–14 (2017).
31. McCarthy, G. et al. Observed interannual variability of the Atlantic meridional overturning circulation at 26.5°N. *Geophys. Res. Lett.* **39**, https://doi.org/10.1029/2012GL052933 (2012).
32. Thorpe, R., Gregory, J., Johns, T., Wood, R. & Mitchell, J. Mechanisms determining the Atlantic thermohaline circulation response to greenhouse gas forcing in a non-flux-adjusted coupled climate model. *J. Clim.* **14**, 3102–3116 (2001).
33. Veres, D. et al. The Antarctic ice core chronology (AICC2012): an optimized multi-parameter and multi-site dating approach for the last 120 thousand years. *Clim. Past* **9**, 1733–1748 (2013).
34. Landais, A. et al. A continuous record of temperature evolution over a sequence of Dansgaard-Oeschger events during Marine Isotopic Stage 4 (76 to 62 kyr BP). *Geophys. Res. Lett.* **31**, 1–4 (2004).
35. Martrat, B. et al. Abrupt temperature changes in the Western Mediterranean over the past 250,000 years. *Science (80-.).* **306**, 1762–1765 (2004).
36. Stommel, H. & Hall, P. Thermohahe convection with two stable regimes of flow. *Tellus* **11**, 224–230 (1961).
37. Petersen, S., Schrag, D. & Clark, P. A new mechanism for Dansgaard-Oeschger cycles. *Paleoceanography* **28**, 1–7 (2013).
38. Li, C. & Born, A. Coupled atmosphere-ice-ocean dynamics in Dansgaard-Oeschger events. *Quat. Sci. Rev.* **203**, 1–20 (2019).
39. Hasumi, H. *CCSR Ocean Component Model (COCO) version 4.0.* CCSR Rep (The University of Tokyo, 2006).
40. Hunke, E. C. & Dukowicz, J. K. An elastic–viscous–plastic model for sea ice dynamics. *J. Phys. Oceanogr.* **27**, 1849–1867 (1999).
41. Cox, P. M. Isopycnal diffusion in a z-coordinate ocean model. *Ocean Model* **74**, 1–5 (1987).
42. Gent, P. R. & Mcwilliams, J. C. Isopycnal mixing in ocean circulation models. *J. Phys. Oceanogr.* **20**, 150–155 (1990).
43. Noh, Y. & Jin Kim, H. Simulations of temperature and turbulence structure of the oceanic boundary layer with the improved near-surface process. *J. Geophys. Res. Ocean.* **104**, 15621–15634 (1999).
44. Nakano, H., Suginohara, N., Nakano, H. & Suginohara, N. Effects of bottom boundary layer parameterization on reproducing deep and bottom waters in a world ocean model. *J. Phys. Oceanogr.* **32**, 1209–1227 (2002).
45. Hasumi, H. & Emori, S. K-1 coupled GCM (MIROC) description. *K-1 Tech. Rep.* **1**, 34, https://ccsr.aori.utokyo.ac.jp/~hasumi/miroc_description.pdf (2004).
46. Oka, A., Hasumi, H., Okada, N., Sakamoto, T. T. & Suzuki, T. Deep convection seesaw controlled by freshwater transport through the Denmark Strait. *Ocean Model* **15**, 157–176 (2006).
47. Hasumi, H., Yasuda, I., Tatebe, H. & Kimoto, M. Pacific bidecadal climate variability regulated by tidal mixing around the Kuril Islands. *Geophys. Res. Lett.* **35**, 1–5 (2008).
48. Weber, S. et al. The modern and glacial overturning circulation in the Atlantic ocean in PMIP coupled model simulations. *Clim. Past* **3**, 51–64 (2007).
49. Otto-Bliesner, B. L. et al. Last Glacial Maximum ocean thermohaline circulation: PMIP2 model intercomparisons and data constraints. *Geophys. Res. Lett.* **34**, 1–6 (2007).

Acknowledgements

Author contributions
A.O. designed the numerical experiment, performed the OGCM simulations, and analyzed the results. H.H. developed the MIROC prototype and contributed to setting up the model simulations. A.A. coordinated the MIROC glacial simulations. S.T. contributed to the interpretation of the model results. Y.Y. and K.K. contributed to the interpretation of ice core record. All of the authors discussed the results and A.O. wrote the paper.

Competing interests
The authors declare no competing interests.

Additional information